

Validation of the burn-up code EVOLCODE 2.0 with PWR experimental data and with a Sensitivity/Uncertainty analysis

F. Álvarez-Velarde*, E.M. González-Romero, I. Merino Rodríguez

CIEMAT, Centro de Investigaciones Científicas, Medioambientales y Tecnológicas, Avda. Complutense, 40 Ed. 17, 28040 Madrid, Spain

ABSTRACT

A validation of the burn-up simulation system EVOLCODE 2.0 is presented here, involving the experimental measurement of U and Pu isotopes and some fission fragments production ratios after a burn-up of around 30 GWd/tU in a Pressurized Light Water Reactor (PWR). This work provides an in-depth analysis of the validation results, including the possible sources of the uncertainties. An uncertainty analysis based on the sensitivity methodology has been also performed, providing the uncertainties in the isotopic content propagated from the cross sections uncertainties. An improvement of the classical Sensitivity/Uncertainty (S/U) model has been developed to take into account the implicit dependence of the neutron flux normalization, that is, the effect of the constant power of the reactor. The improved S/U methodology, neglected in this kind of studies, has proven to be an important contribution to the explanation of some simulation-experiment discrepancies for which, in general, the cross section uncertainties are, for the most relevant actinides, an important contributor to the simulation uncertainties, of the same order of magnitude and sometimes even larger than the experimental uncertainties and the experiment-simulation differences. Additionally, some hints for the improvement of the JEFF3.1.1 fission yield library and for the correction of some errata in the experimental data are presented.

Keywords:

Burn-up code
Code validation
Sensitivity/Uncertainty analysis
Uncertainty propagation

1. Introduction

Computer codes with the burn-up capability to simulate irradiation history have been extensively used on the one hand for understanding the behaviour of current reactors fuel pins under irradiation, especially when dealing with high burn-up simulations achievable in the current nuclear concepts mainly for economic reasons (extending the cycle length). On the other hand, concerning advanced nuclear concepts such as Generation IV fast reactors (and even some Generation III reactors), still without worldwide implementation, the computer simulation has been the most widely used tool to model and evaluate their properties, including reactivity, safety and waste management issues.

The EVOLCODE 2.0 simulation system (Álvarez-Velarde et al., 2007) was developed at CIEMAT with the aim of providing a computer code able of making simulations of current and future reactors in any range of operation and to provide detailed spatial distribution and time evolution of the isotopic composition of fuels and activated materials. Particularly, the capability of making simulations of isotopic evolution in the fuel for nuclear systems with

very diverse characteristics and reaching long fuel burn-ups was focused. For these reasons, the present version of the EVOLCODE system is based upon the MCNPX code (Pelowitz et al., 2009) for the neutronic transport simulation and the ORIGEN code (Croff, 1980) for the depletion calculations. Any version of these codes can be implemented in EVOLCODE 2.0. Alternatively, the user has the option of using MCNP5 code (Brown et al., 2010) for transport and the ACAB code (Sanz et al., 2008) for depletion instead of the base codes to gain additional capabilities.

The code has been validated (mainly for fast neutron systems) up to now by the participation in international code benchmarks (Janczyszyn et al., 2011; Broeders et al., 2010). However, recently an experimental data set focused on Pressurized Light Water Reactors (PWRs) discharge composition has become available. This experiment, the Isotopic Correlation Experiment (ICE) (Koch and Schoof, 1981), was intended for the measure of some actinides and fission products generated after burn-up.

The ICE experimental measurements have been used by different institutions to validate several burn-up codes (with generally high degree of success) (Koch and Schoof, 1981; Cao et al., 2010; Send, 2005), which is the case of MCNPX with the integration of CINDER (Fensin et al., 2006), the deterministic code KAPROS and its burn-up module KARBUS (Broeders et al., 2004) or preliminarily with EVOLCODE 2.0 (Álvarez-Velarde and González-Romero,

* Corresponding author. Tel.: +34 91 346 6731; fax: +34 346 6576.

E-mail address: francisco.alvarez@ciemat.es (F. Álvarez-Velarde).

2011). This work was accomplished in the frame of the IAEA Coordinated Research Project on *Analytical and Experimental Benchmark Analyses of Accelerator Driven Systems* (Broeders et al., 2010). Nevertheless, in these studies only a direct comparison between experimental and simulation data was performed without extensive analysis of the sources of the discrepancies.

In this paper, a Sensitivity/Uncertainty analysis (S/U) has been performed to investigate the sources of the differences between the experimental data and the simulations results, possibly caused by the propagation of the cross sections uncertainties, or by other uncertainty sources that must be taken into account. A detailed description of the results found from the validation of EVOLCODE 2.0 using the ICE measurements has also been included.

This work is framed within the ANDES project (ANDES, 2010) (Accurate Nuclear Data for nuclear Energy Sustainability, 7th Framework Programme of the European Union). Its results will allow providing some guidelines in order to advise additional strategies for cross section uncertainty reduction.

2. Methodology

2.1. Description of EVOLCODE 2.0

EVOLCODE 2.0 is a combined neutronics and burn-up evolution simulation code aimed for the description of the burn-up evolution of either critical or subcritical reactors operating in any neutron spectrum regime. The code is able to estimate a great variety of nuclear reactor parameters, in particular, the isotopic composition evolution of the fuel in a nuclear reactor.

Burn-up problems are solved by EVOLCODE 2.0 using an time-interval method consisting in the successive calculation of first the neutron flux for fixed material densities at a given time and later the depletion of these densities, using the hypothesis of constant neutron flux. Given that the validity of the hypotheses of constant properties is limited in the irradiation time, several calculations are needed to solve the system for the whole irradiation period. Each iteration, corresponding to a partial irradiation period, is called an EVOLCODE cycle. The cycle data flow of the EVOLCODE procedure is shown in Fig. 1.

In the present version of the code (Álvarez-Velarde et al., 2007), the neutron transport calculations are implemented by the general

Monte Carlo N-Particle Transport Code MCNPX or alternatively by the MCNP5 code. The Isotope Generation and Depletion Code ORIGEN currently implements the depletion of the geometry zones, requested by the user, although the code ACAB has also been implemented in the EVOLCODE 2.0 system to provide results uncertainties and to enlarge the number of nuclear reactions taken into account by the irradiation calculations. Both ORIGEN and ACAB are point-depletion and radioactive decay computer codes, and share the main computational mechanism called the transition matrix method (Croff, 1983). The user chooses which depletion code or version of MCNP/X is used in the simulations.

As it will be shown in the following, many of the characteristics of the programming of EVOLCODE 2.0 are aimed to deal with the proper implementation of the applied hypotheses so that the precision in the calculation is optimized.

The space dependence of the neutron flux is determined by the MCNPX cell definition, together with the entire geometry definition, allowing an important degree of the heterogeneity description in the reactor core model. The energy dependence is obtained by means of the energy spectrum of the neutron flux for each of these cells. On the one hand, the neutron flux is normalized so that the depletion is simulated using the proper value of the system thermal power. On the other hand, the neutron flux energy spectra are used for creating (outside MCNPX) one-group effective cross-section libraries for ORIGEN. Even using a largely detailed number of energy groups (around 30,000), EVOLCODE 2.0 performances reduce the computer time by one-two dozens while providing results with the same accuracy (Álvarez-Velarde, 2011) as if the simulation was made using the MCNPX burn-up capability. This fact has also been observed in other burn-up codes using this methodology (Haeck and Verboomen, 2007).

EVOLCODE is pushed to use the same basic libraries that MCNP does, so that the consistency in the data treatment is ensured. From these basic libraries, the information of those reactions suitable for ORIGEN and available in the database is selected, disregarding the information about elastic collisions. Additionally, since isomers may have very different half-lives and reaction cross sections compared with the ground state isotope (leading to different transmutation chains), the information of the isomer producing reactions is provided to the code by a separated file, ENDF File 9, containing the information of the branching ratios, i.e.,

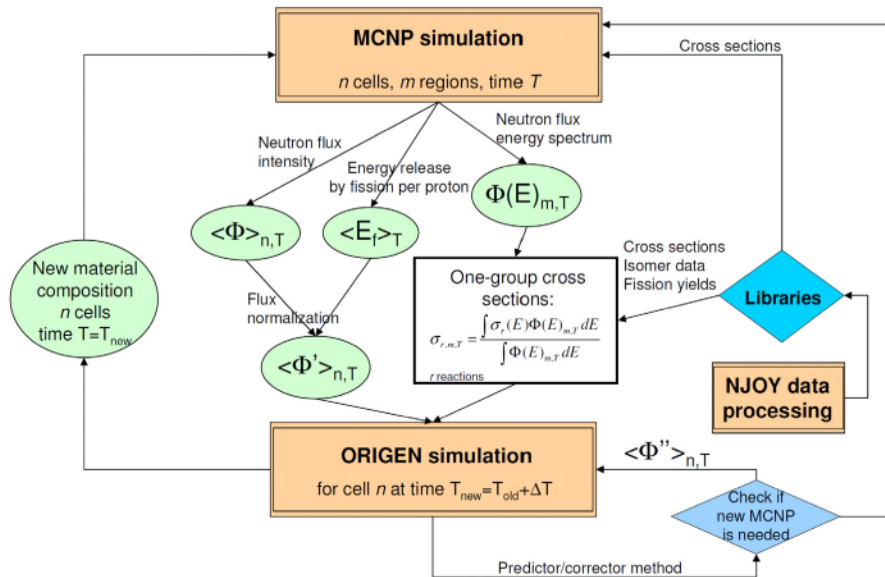


Fig. 1. EVOLCODE2 cycle data flow scheme.

fractions of the cross section in the reaction which produces the excited/isomer states in the daughter nucleus. Finally, the fission yields library is also supplied to the code as an external sublibrary. Currently, sublibraries are defined for neutron-induced fission product yields and for yields from spontaneous fission. Besides, independent and cumulative¹ yields are included in the sublibrary. EVOLCODE 2.0 only considers neutron-induced independent fission product yields since this is the data required by the depletion code.

Inside each cell, the neutronic and material properties are considered constant (in time but also homogenised in space). Hence a discretization in relatively large cells might cause that the neutron flux is not really constant inside the cell. On the contrary, a relatively large number of small cells might need unacceptably large computer times. EVOLCODE 2.0 provides a methodology to find a proper compromise between accuracy and requirements on computing time and resources (Álvarez-Velarde, 2011).

The cycle length must be limited to keep to a good approximation the condition of constant neutron flux in the cell along time. Indeed, the neutron flux varies along the irradiation (with the evolution of the materials), and it might reach large deviations from the assumed constant value in case of systems with high or very high burn-up. EVOLCODE uses a predictor/corrector method to optimize the cycle length avoiding too large irradiation periods. This method is also used to guarantee that the reactor power is kept constant, at least with a deviation smaller than a certain value specified by the user.

The isotopic composition evolution is calculated with ORIGEN separately for each evolving cell. The materials evolution can be estimated for the entire reactor or for only a small amount of cells where the isotopic evolution is desired by the user. For those cells chosen by the user, ORIGEN performs irradiation procedures using the one-group cross section library created by EVOLCODE.

The burn-up evolution of the whole reactor is estimated as the union of the burn-up evolution of the different evolving cells. With the new reactor materials composition available after a partial irradiation, it is possible to obtain the new neutronic parameters of the system with MCNPX and then the evolution of the materials isotopic composition for a new successive partial irradiation step. The whole irradiation is simulated after several cycles and the final solution is estimated as a piecewise-defined function for both the neutron flux and the material isotopic compositions.

2.2. Sensitivity/Uncertainty analysis

2.2.1. Basis

The principles of Sensitivity/Uncertainty (S/U) analysis are well known and documented and have been applied to study the impact of the nuclear data uncertainties on performance parameters such as the irradiated fuel isotopic composition (Aliberti et al., 2004; García-Herranz et al., 2010). We will simply summarize here some relevant information as starting point of our work. Let $\vec{X}(t) = (X_1(t), X_2(t), \dots, X_n(t))$ be the space-averaged nuclide composition of a material at time t . The net balance of each isotope X_k can be described by the Bateman equations that expressed in a matrix notation are

$$\frac{d\vec{X}}{dt} = \mathbf{B}(\Phi) \cdot \vec{X}, \quad (1)$$

where $\mathbf{B}(\Phi)$ is the matrix involving the averaged cross sections, decay constants and the neutron flux Φ , and t is the irradiation time. The formal solution of this equation, for constant flux and effective cross sections, is

$$\vec{X}(t) = e^{\mathbf{B}(\Phi)t} \vec{X}(0). \quad (2)$$

In this work, we are only interested in a small group of actinides, so we will merely refer to a small group of q nuclides. The evolution of these isotopes will depend only on a particular set of m cross sections that can be grouped as $\vec{\sigma} = (\sigma_1, \sigma_2, \dots, \sigma_m)$, covering these isotopes and the nuclear reactions for capture and fission. Other possible contributions like (n,xn) are included in the simulations but not in the S/U analysis. Let us assume that the other parameters in the problem (other cross sections, decay parameters, ...) are known and constant, and that the analysis is made for a period of time between 0 and t . Each element X_k is hence a function of the cross section vector $\vec{\sigma}$, $X_k = X_k(\vec{\sigma})$, where t will no longer be explicitly written in the formulation for simplicity. The goal is then to analyse how the uncertainties in the cross sections are transmitted to the final nuclide composition estimations \vec{X} .

The variation in \vec{X} due to a variation in $\vec{\sigma}$ can be expressed as

$$\Delta X_k = \sum_{l=1}^G \sum_{j=1}^m S_{kj}^l \Delta \sigma_j^l, \quad (3)$$

where the sensitivity coefficients S_{kj}^l are given by

$$S_{kj}^l = \frac{\partial X_k}{\partial \sigma_j^l}. \quad (4)$$

In these expressions, we have introduced superscript l that takes into account that the nuclear data uncertainties $\Delta \sigma_j^l$ are usually provided for a certain number of G energy groups. Taking into account that the reaction cross sections always appear explicitly in the form $\sigma_j^{\text{eff}} = \sum_{l=1}^G \sigma_j^l \Phi^l / \sum_{l=1}^G \Phi^l$, it is possible to write

$$S_{kj}^l = \frac{\partial X_k}{\partial \sigma_j^{\text{eff}}} \frac{\partial \sigma_j^{\text{eff}}}{\partial \sigma_j^l} = \frac{\partial X_k}{\partial \sigma_j} \frac{\Phi^l}{\sum_{l=1}^G \Phi^l} \equiv S_{kj} \frac{\Phi^l}{\sum_{l=1}^G \Phi^l} \quad (5)$$

so that the variation in \vec{X} becomes

$$\Delta X_k = \sum_{j=1}^m S_{kj} \Delta \sigma_j^{\text{eff}}. \quad (6)$$

Furthermore, the cross sections corresponding to different energy groups are affected of cross-correlations and even the cross sections of different reactions show significant correlations in some cases. Taking into account these correlations, the uncertainties can be represented by means of a variance-covariance matrix,

$$C = \begin{pmatrix} C_{11} & C_{12} & \dots & C_{1m} \\ C_{21} & C_{22} & \dots & C_{2m} \\ \dots & \dots & \dots & \dots \\ C_{m1} & C_{m2} & \dots & C_{mm} \end{pmatrix}, \quad (7)$$

where each C_{ij} represents a $G \times G$ matrix accounting for the G energy groups.

Once the sensitivity coefficients and the uncertainties in the variance-covariance matrix are known, the variance of the nuclide composition \vec{X} can be evaluated as follows:

$$\Delta^2 X_k = S_k^T C S_k \quad (8)$$

2.2.2. Implicit dependence of the neutron flux normalization on the cross sections

The dependence of X_k on the cross sections comes on the one hand from their explicit appearance in the solution of the Bateman equations for isotope k and, on the other hand, from the implicit dependence of the neutron flux on the cross sections. The implicit dependence has been usually neglected in previous works related to uncertainties propagation in fast systems (Aliberti et al., 2004; García-Herranz et al., 2008) considering that the feedback from flux and spectrum changes along irradiation is very low. However, in thermal reactors where the initial fuel content is made of ura-

¹ Number of atoms of a specific nuclide produced directly (as independent fission yield) and via decay of precursors.

nium, the neutron flux varies significantly along burn-up in the thermal region due to the appearance of ^{239}Pu and ^{240}Pu , having strong capture resonances at 0.3 eV and 1 eV, respectively. Due to this reason, the possibility that the implicit dependence of the neutron flux normalization could impact significantly the final uncertainty of some isotopes is explored here.

However, in this work, only a part of the implicit dependence is considered as described below. Additional dependences due to the energy dependence of the neutron flux with the energy dependence of the reaction and scattering cross sections could also affect the results and are not fully included in this analysis.

In order to consider the implicit dependence we take into account that the energy-integrated value of the neutron flux is linked to the reactor power, which is a measure of the energy release by fission per unit time. The energy release by fissions in the whole reactor after the complete irradiation period can be estimated with the burn-up, which is measured in practice by means of the amount of ^{148}Nd (Furcola, 1996), represented as $X^{\text{Nd-148}}$ below. This amount is equal to the number of fissions per isotope times the corresponding fission yield:

$$X^{\text{Nd-148}} = \iint \sum_k \sigma_{fk}(E) Y_k^{\text{Nd-148}}(E, t) X_k(t) \Phi(E, t) dE dt \quad (9)$$

In this expression, $\sigma_{fk}(E)$ represents the fission cross section of fissile isotope k , $X_k(t)$ is the amount of fissioning specie k , and $Y_k^{\text{Nd-148}}(E, t)$ is the cumulative fission product yield of ^{148}Nd .

Making the convolution of the microscopic fission cross section with the neutron flux, the energy dependence can be integrated as

$$X^{\text{Nd-148}} = \int \sum_k \bar{\sigma}_{fk} Y_k^{\text{Nd-148}} X_k(t) \Phi(t) dt, \quad (10)$$

where $\bar{\sigma}_{fk}$ is the one-group effective fission cross section of isotope k . To achieve this, we have assumed that $Y_k^{\text{Nd-148}}(E, t) = Y_k^{\text{Nd-148}}$ (independent of energy spectrum and time for the ranges of spectra in the problem), which is rather correct for ^{148}Nd cumulative fission product yields from both ^{235}U and ^{239}Pu .

If the burn-up of a reactor cycle is not high, the neutron flux varies reasonably slowly so we take its average value Φ as representative for the whole irradiation period:

$$\Phi = \frac{X^{\text{Nd-148}}}{\int \sum_k \bar{\sigma}_{fk} Y_k^{\text{Nd-148}} X_k(t) dt}. \quad (11)$$

This equation states that the neutron flux depends on the fission cross sections, the amounts of fissile materials (that correspondingly depend on some cross sections) and the ^{148}Nd fission yields. Considering only fissions from ^{235}U and ^{239}Pu , Eq. (9) becomes

$$X^{\text{Nd-148}} = \frac{U_0^5 \sigma_f^5 Y^5}{\sigma_c^5 + \sigma_f^5} \left(1 - e^{-(\sigma_c^5 + \sigma_f^5) \Phi t} \right) + \frac{U_0^8 \sigma_f^8 Y^8}{(\sigma_c^8 - \sigma_c^9 - \sigma_f^9) (\sigma_c^9 + \sigma_f^9)} \times \left(\sigma_c^8 - \sigma_c^9 - \sigma_f^9 + (\sigma_c^9 + \sigma_f^9) e^{-\sigma_c^8 \Phi t} - \sigma_c^8 e^{-(\sigma_c^9 + \sigma_f^9) \Phi t} \right) \quad (12)$$

where superscripts 5, 8 and 9 refer respectively to isotopes ^{235}U , ^{238}U and ^{239}Pu (the "eff" superscript has been removed in all cross sections for simplicity). This equation has been used to derive the expressions of $\partial \Phi / \partial \sigma_j$ appearing in Eq. (5) when the implicit dependence of the neutron flux normalization on the cross sections is considered. Besides, the uncertainties in the cumulative fission product yields Y^5 and Y^9 have also been considered in this work, since they are provided in the data libraries.

2.3. The isotope correlation experiment

2.3.1. Description of the experiment

The European Safeguards Research and Development Association (ESARDA) working group on Isotopic Correlation Techniques (ICT) and Reprocessing Input Analyses performed in the 1970s an experiment to check the feasibility of the ICT. This experiment was developed at the Obrigheim nuclear power plant and was called Isotopic Correlation Experiment (ICE) (Koch and Schoof, 1981).

The objectives of this experiment, counting with the participation of several European institutions, were the determination of the accuracy of the measurement technique, the identification of additional required information and safeguard-related issues. In order to achieve these objectives, several fuel assemblies were chosen from the spent fuel after the normal operation of the Obrigheim power plant (KWO). After that, isotopic analyses were performed at the reprocessing plant WAK at Karlsruhe, measuring the amount of some actinides and fission products present in the spent fuel.

The experiment was conducted at normal operation of the plant. Ten consecutive dissolution batches each making up half of the fuel assembly were chosen for the experiment. The geometrical data of the pins used for the experiment have been obtained from bibliography (Send, 2005). The UO_2 pin (with a stoichiometry of $2.00 \pm 0.01\%$) had an external radius of 0.465 cm. Its average operation temperature was 1028 K. The cladding material was zirconium with outer radius of 0.535 cm and average operation temperature of 605 K. The moderator was water at a temperature of 572 K averaged over the fuel channel.

The uranium content (approximately 311 kg of UO_2 per assembly with an uncertainty of 0.4%) was supplied by KWO, as well as the irradiation history and the boron concentration in water, both in 29 different time steps for the total of around 30 GWd/tU. This information is available in bibliography (Send, 2005).

Post-irradiation analyses performed at the reprocessing plant included the measurement of the concentration of uranium isotopes (^{235}U , ^{236}U and ^{238}U), plutonium isotopes (^{238}Pu to ^{242}Pu), some fission products and minor actinides (Am, Cm). ^{148}Nd were used as an indicator of the burn-up. There were no measurements of head-end losses.

2.3.2. Simulation details

The reference geometrical and thermal hydraulic settings used by EVOLCODE 2.0 to simulate ICE are included in Table 1 (Koch and Schoof, 1981; Send, 2005; Broeders, 1992). The simulation model has consisted in a pin design of an Obrigheim 14×14 PWR, considering a fuel pellet, cladding, and moderator and with reflecting boundary surfaces. The fuel pellet has been divided radially in 25 cells with different thicknesses for taking into account the larger creation of plutonium at the pin periphery.

Table 1
ICE simulation settings.

Parameter	Value
Pin radius	0.465 cm
Cladding thickness	0.07 cm
Pin side length	1.498 cm
Fuel density	0.0681 at/cm-barn
Cladding density	0.0432 at/cm-barn
Moderator density	0.0721 at/cm-barn
Fuel temperature	1200 K
Cladding temperature	600 K
Water temperature	600 K
Initial ^{235}U enrichment	3.1%

Reflecting axial boundaries have also been implemented in the model.

The pin is surrounded by a Zr cladding. The moderator is borated water. Thermal $S(\alpha,\beta)$ tables for hydrogen in light water at 600 K have been used in the moderator. The volume ratio of moderator to fuel has been set to $V_m/V_f = 1.978$, to account for the additional water contained in the control rod tubes.

An alternative simulation with a more sophisticated model has also been performed to explore the effect of the geometrical model. This alternative model describes the experiment, as shown in Fig. 2, as a fuel assembly horizontal slice with a pin-pitch of 1.43 cm, and again with reflecting boundary surfaces. In this model, 125 cells with different isotopic evolution have been considered to take into account the rim effect and the different neutron spectra of different pins inside the assembly. No S/U analysis has been performed to this model.

A total of 53 EVOLCODE cycles have been performed for an adequate simulation of the ICE experimental irradiation history, including 11 cycles without irradiation (decay only). MCNPX version 2.7 and ORIGEN version 2.2 have been used as part of the EVOLCODE 2.0 system (together with the JEFF3.1.1 library for cross sections, isomer branching ratios, fission product yields and decay data) to simulate this experiment.

For the S/U analysis, we have used the COMMARA covariance library (Herman et al., 2011) including the information of the relative uncertainty in the cross sections and the correlations (for the 33 energy groups included in Table 2) for the following isotopes and reactions: ^{235}U (n,f), ^{235}U (n, γ), ^{235}U fission-capture cross correlations, ^{236}U (n, γ), ^{238}U (n, γ), ^{238}Pu (n, γ), ^{238}Pu (n,f), ^{239}Pu (n,f), ^{239}Pu (n, γ), ^{239}Pu fission-capture cross correlations, ^{240}Pu (n, γ), ^{241}Pu (n, γ), ^{241}Pu (n,f) and ^{237}Np (n,f). According to Table 2, the thermal region only contains two energy groups. Although this might be insufficient to fully describe the energy groups causing uncertainties in problems with thermal spectra (such as a light water-cooled reactor), this work can provide a motivation to improve the database subdivision in groups and an improved methodology to be used in S/U analysis now and in the future when more detailed databases become available.

Although the COMMARA library is based on the ENDF/B-VII library and the burn-up simulation has been done using the JEFF3.1.1 library, both libraries are based essentially on the same basic nuclear data so it is a reasonable approximation to use the COMMARA covariance for a JEFF3.1.1 calculation. The neutron flux

energy spectrum and the reaction rates (for the 33 energy groups) used in the S/U analysis have been obtained by means of MCNPX.

3. Comparison between experimental and predicted results

3.1. Actinides

This section includes the validation results of the simulation with EVOLCODE 2.0 of the ICE experiment. These results are shown as a comparison of the prediction for the number density (atoms per initial metal atoms, IMA) of each isotope with experimental data, as functions of the burn-up. The evolution with burn-up of the number density of the studied actinides can be found at Figs. 3–10. For this validation, the burn-up has been estimated in EVOLCODE by means of the ASTM standard procedure described in the bibliography (Furcola, 1996), using ^{148}Nd as a burn-up indicator by means of the number of fissions estimated by the code.

The experimental procedure for the measurement of the burn-up values involves an inaccuracy of $\pm(3-5)\%$. This can be deduced from experiments in which the burn-up has been measured using several methods and/or by several laboratories (Barbero et al., 1979). Since the burn-up is used to compare the experiment with the simulation results, a 4% error bar will be assigned to this magnitude in the figures.

Experimental data has been obtained as averaged values coming from measurements made by four different institutions (Koch and Schoof, 1981). The dispersion between the data of the four laboratories has been expressed as variation coefficients and computed as the variance of the mean value. The variation coefficients of the averaged data are also provided in this reference. These values have been taken as uncertainties in the experimental number density and can be found in the second column of Table 3. This table also shows (third column) the averaged relative difference between the experimental data and the simulation results from EVOLCODE 2.0. The results of the S/U analysis are also included in the table and will be described in detail below.

It should be noted that, for comparison reasons, the experimental results were corrected to the date of the reactor shutdown. This is the case of ^{241}Pu and ^{238}Pu , and some fission products that have not been identified in the bibliography. In-pile decay corrections, however, were not applied (Koch and Schoof, 1981). For this reason, the final 53rd cycle (365 days of cooling decay) has been disregarded and not shown in the figures.

There is a very good agreement between the simulation and the experimental data, especially for the actinides with larger amount (number density larger than 10^{-3}). In particular for the uranium isotopes, the agreement is very good for ^{235}U (shown in Fig. 3) and excellent for ^{238}U (Fig. 5). The averaged discrepancy between the simulation and the experimental data is 2.3% for ^{235}U (compatible with error bars) and 0.023% for ^{238}U . The case of ^{236}U can be seen in Fig. 4. For this nuclide, discrepancies around 4–6% way beyond experimental uncertainties can be found. However, our simulation provided results very similar to the numerical simulations obtained in the past with MCNPX/CINDER (Cao et al., 2010). According to this reference, one of the possible factors inducing this discrepancy might be the inconsistency and inaccuracy in the ^{235}U capture cross section databases in the energy range of 30 keV to 1 MeV above the resonance range, showing a 10% discrepancy in the capture cross section between libraries. This special case will be studied in detail in the next sections.

For the plutonium isotopes, the agreement between the simulation and the experimental data is very good as well. Fig. 7 shows the comparison between predicted and experimental data for ^{239}Pu . Small sharp variations that can be seen in the simulation curve correspond to radioactive decay-only periods and forthcom-

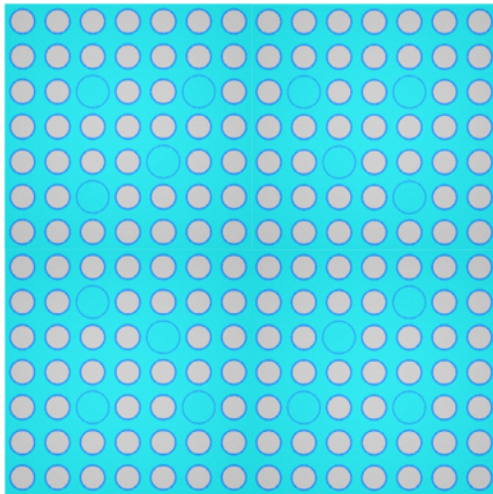


Fig. 2. Schematic view of the fuel assembly model for the alternate simulation.

Table 2
Energy groups of the COMMARA covariance library.

Group	Energy interval upper limit (eV)	Group	Energy interval upper limit (eV)	Group	Energy interval upper limit (eV)
1	1.96E+07	12	6.74E+04	23	3.04E+02
2	1.00E+07	13	4.09E+04	24	1.49E+02
3	6.07E+06	14	2.48E+04	25	9.17E+01
4	3.68E+06	15	1.50E+04	26	6.79E+01
5	2.23E+06	16	9.12E+03	27	4.02E+01
6	1.35E+06	17	5.53E+03	28	2.26E+01
7	8.21E+05	18	3.35E+03	29	1.37E+01
8	4.98E+05	19	2.03E+03	30	8.32E+00
9	3.02E+05	20	1.23E+03	31	4.00E+00
10	1.83E+05	21	7.49E+02	32	5.40E-01
11	1.11E+05	22	4.54E+02	33	1.00E-01

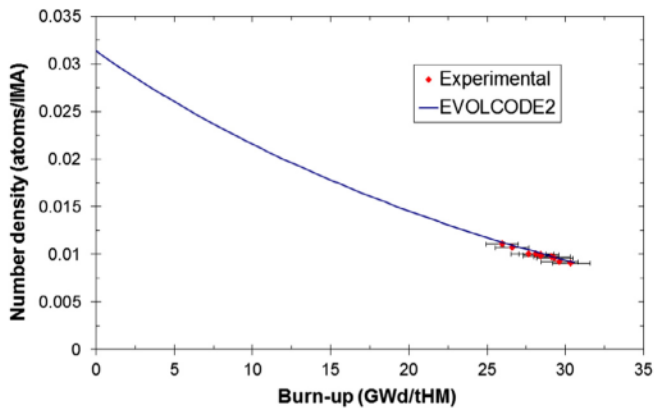


Fig. 3. Comparison of ^{235}U number densities obtained with EVOLCODE 2.0 and experimental data as function of burn-up.

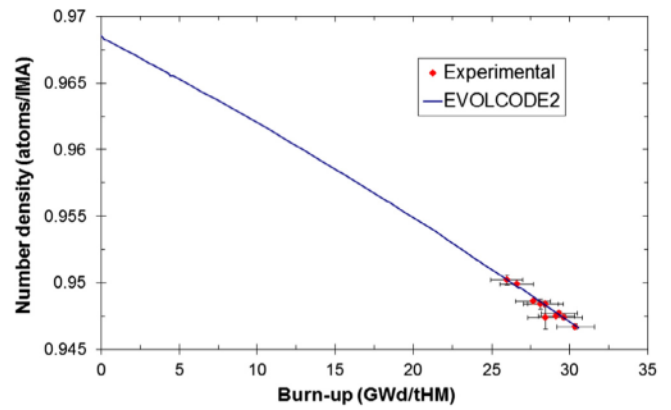


Fig. 5. Comparison of ^{238}U number densities obtained with EVOLCODE 2.0 and experimental data as function of burn-up.

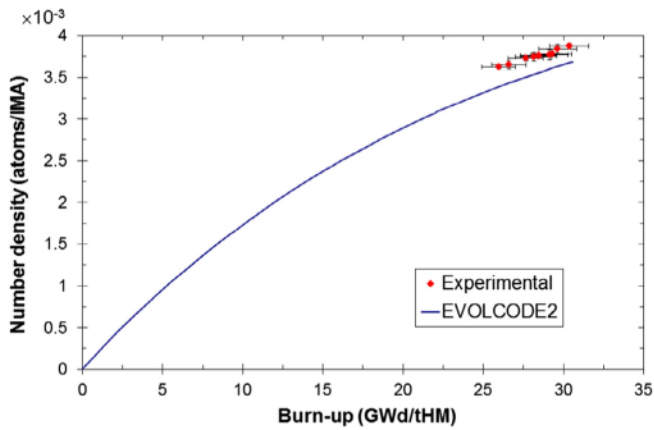


Fig. 4. Comparison of ^{236}U number densities obtained with EVOLCODE 2.0 and experimental data as function of burn-up.

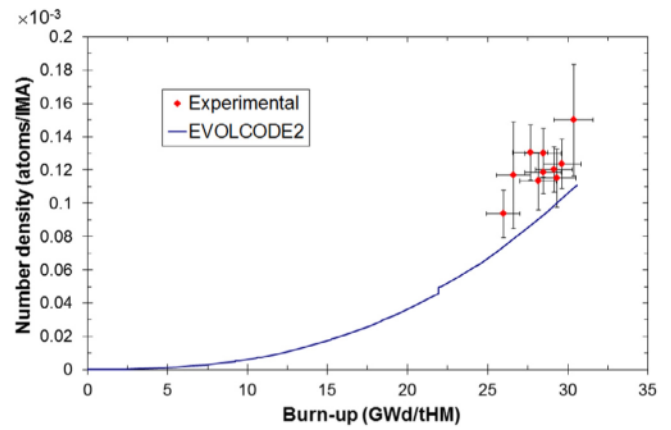


Fig. 6. Comparison of ^{238}Pu number densities obtained with EVOLCODE 2.0 and experimental data as function of burn-up.

ing irradiation periods. Accumulated ^{239}U and ^{239}Np decay to ^{239}Pu during these decay-only periods, causing the small sharp increase. Later, when irradiation continues after the decay-only period, a small decrease appears in the ^{239}Pu amount until equilibrium is regained in the amount of ^{239}U (and ^{239}Np) by captures in ^{238}U . Differences between calculated and experimental data are smaller than 2.5% in almost all points (average value of 1.9%), meaning that the build-up of this isotope is simulated accurately with EVOLCODE 2.0.

Fig. 8 shows the evolution with burn-up of ^{240}Pu , for which the simulation curve fit very well with experimental data. The largest simulation-experiment difference can be found at a burn-up of

28.46 GWd/tHM with a value of 4.3% while the averaged difference is 1.2%. For ^{241}Pu , as shown in Fig. 9, differences are smaller than 6% for all the points (but compatible with experimental error bars) with an averaged difference of 2.7%. For the isotopes with very small amount, the one with the largest deviations is ^{238}Pu (−24%). A high dispersion in the experimental data can be however seen for this isotope. Considering this, the deviation between the simulation and experimental results would range from 1.5 to 2 times the experimental data fluctuations (rms). Similar results could be found in other simulations of this experiment involving MCNPX/CINDER or KAPROS (Send, 2005), or the other isotope with low abundance (^{242}Pu), the experimental value is underestimated

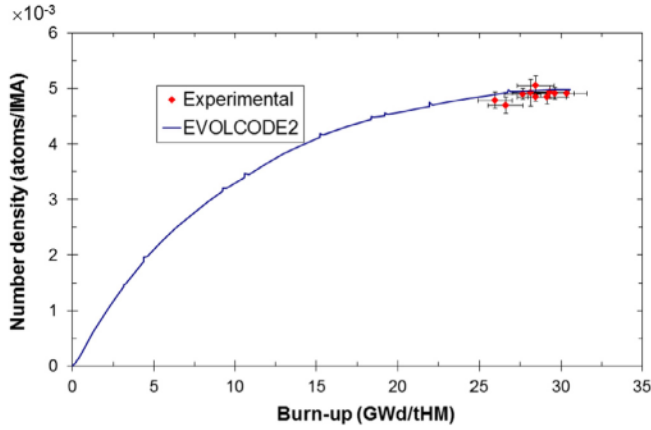


Fig. 7. Comparison of ^{239}Pu number densities obtained with EVOLCODE 2.0 and experimental data as function of burn-up.

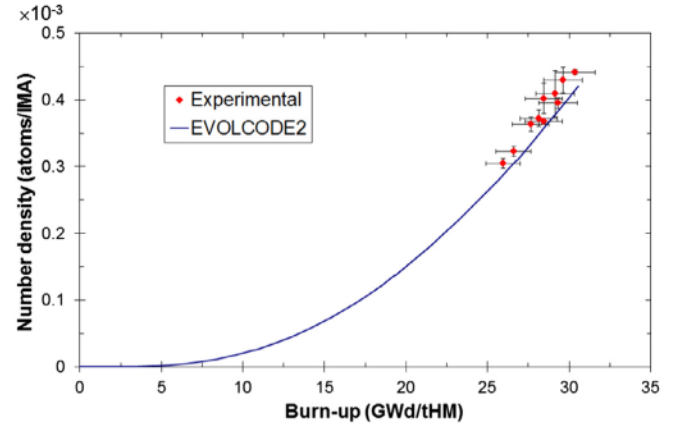


Fig. 10. Comparison of ^{242}Pu number densities obtained with EVOLCODE 2.0 and experimental data as function of burn-up.

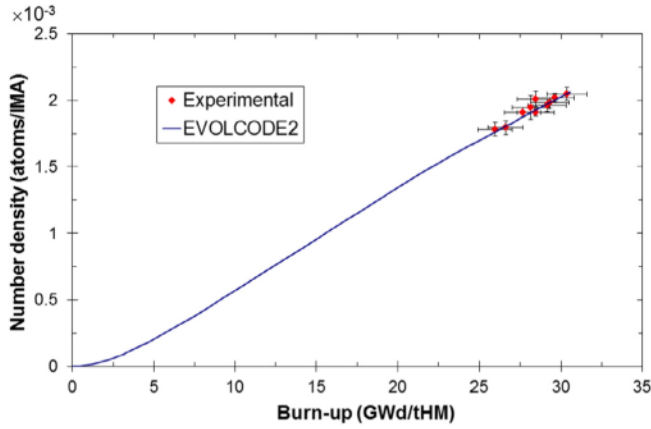


Fig. 8. Comparison of ^{240}Pu number densities obtained with EVOLCODE 2.0 and experimental data as function of burn-up.

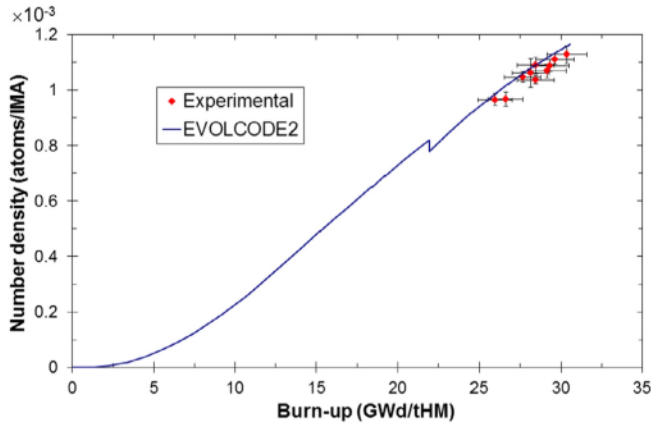


Fig. 9. Comparison of ^{241}Pu number densities obtained with EVOLCODE 2.0 and experimental data as function of burn-up. Sharp decreases (mainly seen at 22 GWd/tHM) correspond to the decay of ^{241}Pu in periods of radioactive decay only.

by around 6.7%, but compatible with experimental error bars in most points. This nuclide is not present in Table 3 because it is not included in the S/U analysis.

We have only analysed U and Pu isotopes, although results for Am and Cm isotopes have been delivered as well and can be seen in Figs. 11–14. The reason for not considering Am and Cm isotopes

in the analysis is that their experimental error bars were not provided. These experimental errors are expected to be high, similar to the ones of ^{238}Pu , due to their small amount. However, we have found similar results to those published in bibliography for these isotopes (Cao et al., 2010).

3.2. Fission products

The ICE experiment also included the measurement of the isotopic atom ratios of some relevant fission products from elements Kr, Xe and Nd, and the $^{134}\text{Cs}/^{137}\text{Cs}$ activity ratio. The evolution with burn-up of these ratios can be found at Figs. 15–18. Again, ^{148}Nd was used as burn-up indicator. Since experimental data has been measured by only one institution (Koch and Schoof, 1981) and experimental errors were not provided, these figures do not show any error bars but our estimation (obtained by means of the dispersion between adjacent points) is that the uncertainty is of the order of magnitude of some 3%.

Concerning Kr isotopes atom ratios, shown in Fig. 15, the simulation underestimates the experimental result by $\sim 18\%$ for both $^{84}\text{Kr}/^{83}\text{Kr}$ and $^{84}\text{Kr}/^{86}\text{Kr}$ ratios and by $\sim 90\%$ for $^{83}\text{Kr}/^{86}\text{Kr}$. However, these experimental ratios are incoherent. If we divide $^{84}\text{Kr}/^{86}\text{Kr}$ ratio between $^{84}\text{Kr}/^{83}\text{Kr}$ ratio, we should obtain $^{83}\text{Kr}/^{86}\text{Kr}$ value. According to experimental data, this division should equal around 0.24. Instead, published experimental values for $^{83}\text{Kr}/^{86}\text{Kr}$ ratio are around 2.4, making us believe that there is a mistake in the transcription of the experimental data by a factor of ten. Considering this factor, the simulation results and the modified experimental data would show a discrepancy of only -1.24% for the $^{83}\text{Kr}/^{86}\text{Kr}$ atom ratio.

The different results obtained for the Kr isotope ratios lead us to explore the possibility that the fission product yields leading to some of these Kr isotopes could be improved. Let us consider the cumulative fission product yields from the JEFF3.1.1 library, although this value is not used by the code, which only uses independent fission yields. According to the library, the $^{84}\text{Kr}/^{83}\text{Kr}$ ratio equals 1.84. Since the ^{83}Kr capture cross is around 200 barn in thermal spectra, the $^{84}\text{Kr}/^{83}\text{Kr}$ experimental atom ratio must be larger than the fission yield theoretical ratio (in agreement with the simulation and the experimental results). Since the $^{84}\text{Kr}/^{83}\text{Kr}$ ratio is underestimated by EVOLCODE, this might mean that the fission yields values of the library could overestimate the ^{83}Kr fission yield or underestimate the ^{84}Kr fission yield. On the other hand, the $^{84}\text{Kr}/^{86}\text{Kr}$ theoretical ratio from the cumulative value equals ~ 0.51 (close to the simulation results) and no large cross sections are applicable to these isotopes. Since the $^{84}\text{Kr}/^{86}\text{Kr}$ ratio is also

Table 3

Results of the application of the COMMARA covariance data to the ICE simulation with EVOLCODE 2.0. Differences have been calculated using the absolute value. Negative signs represent underestimation regarding experimental data.

Isotope	Experimental data uncertainty (%)	Averaged difference (%) between EVOLCODE and experiment		Uncertainty (%) due to cross sections	
		Pin model	Assembly model	Classical approach	Neutron flux normalization
^{235}U	0.65	2.3	1.8	0.35	1.2
^{236}U	0.92	-5.5	-5.4	1.8	2.2
^{238}U	0.028	0.023	0.025	0.028	0.030
^{238}Pu	15	-24	-24	6.0	6.2
^{239}Pu	2.6	1.9	-1.2	1.2	1.2
^{240}Pu	2.5	-1.2	-1.2	1.9	1.9
^{241}Pu	2.4	2.7	1.4	2.4	2.8

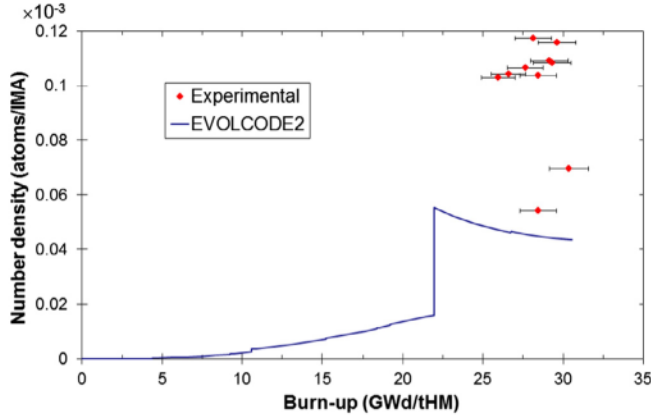


Fig. 11. Comparison of ^{241}Am number densities obtained with EVOLCODE 2.0 and experimental data as function of burn-up.

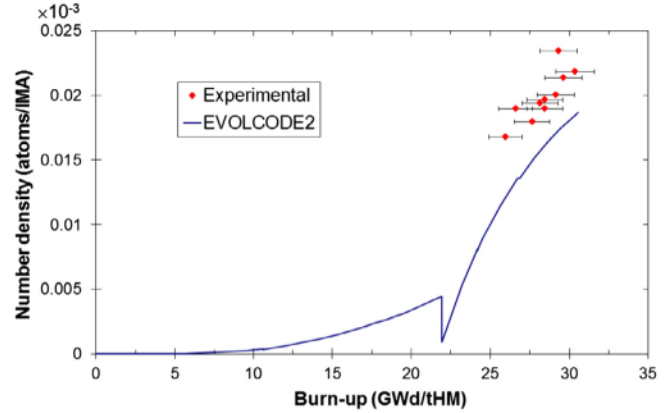


Fig. 13. Comparison of ^{242}Cm number densities obtained with EVOLCODE 2.0 and experimental data as function of burn-up.

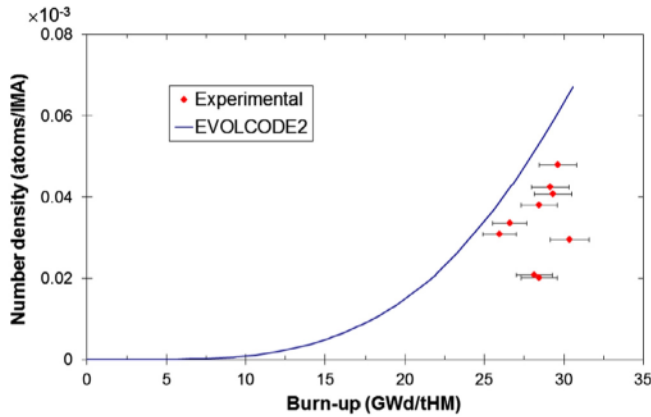


Fig. 12. Comparison of ^{243}Am number densities obtained with EVOLCODE 2.0 and experimental data as function of burn-up.

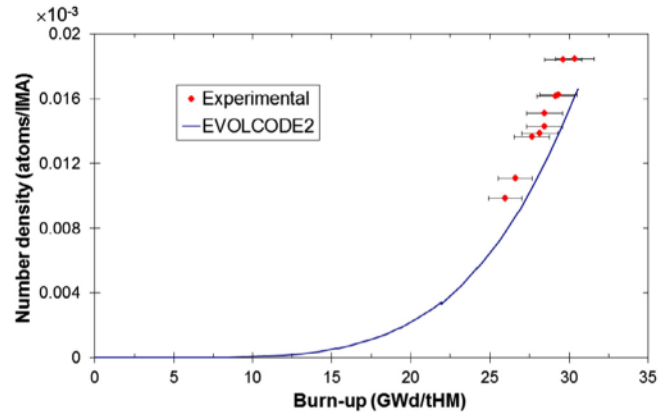


Fig. 14. Comparison of ^{244}Cm number densities obtained with EVOLCODE 2.0 and experimental data as function of burn-up.

underestimated by the simulation, this might suggest that the fission product yields leading to ^{84}Kr could be underestimated in the library. This rationale is finally strengthened by the fact that the $^{83}\text{Kr}/^{86}\text{Kr}$ atom ratio, with no presence of ^{84}Kr has a discrepancy of only $\sim 1.24\%$ (considering the abovementioned erratum).

Fig. 16 shows a very good agreement between the simulation with EVOLCODE and the ICE experimental data for the Xe isotope atom ratios, for which the averaged discrepancies between simulation and experimental data is around or less than 6%. For Nd atom ratios (Fig. 17) the agreement is excellent for atom ratios $^{146}\text{Nd}/^{145}\text{Nd}$, $^{143}\text{Nd}/^{148}\text{Nd}$, $^{145}\text{Nd}/^{148}\text{Nd}$, and $^{146}\text{Nd}/^{148}\text{Nd}$, with averaged discrepancies less than 2%. However, the isotope atom ratio $^{144}\text{Nd}/^{148}\text{Nd}$ shows a discrepancy of -24% . Although the experiment description states that experimental results were cor-

rected to the date of the reactor shutdown for some (unidentified) fission products, one of the parents of ^{144}Nd , ^{144}Ce , has a relatively long half-life of 284.8 d. Results might suggest that the amounts of ^{144}Nd at the time of the experimental measure were not corrected, since the values of $(^{144}\text{Nd}+^{144}\text{Ce})/^{148}\text{Nd}$ taken from the simulation show a discrepancy with experimental data of only -4% .

Finally, Fig. 18 shows an excellent agreement for the $^{134}\text{Cs}/^{137}\text{Cs}$ activity ratios, since the averaged discrepancy between the simulation values and experimental data is around 3%, not considering the isolated point located at (29.32 GWd/tHM, 1.77) in the figure.

4. Sensitivity/Uncertainty analysis

In the previous section we have found that EVOLCODE 2.0 reproduces the ICE experimental data very satisfactorily. However, for some actinides the obtained mass differences between the sim-

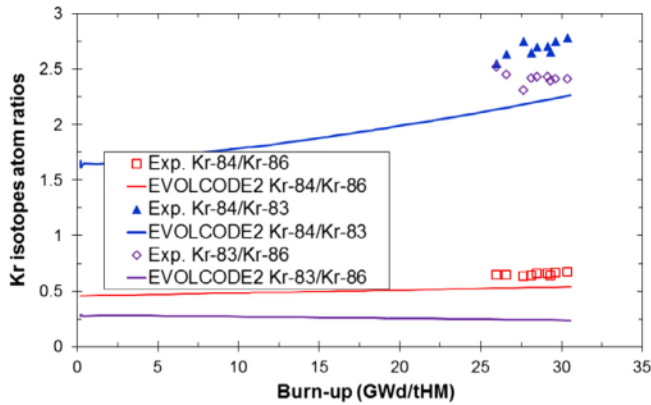


Fig. 15. Comparison of Kr isotopes atom ratios obtained with EVOLCODE 2.0 and experimental data as function of burn-up.

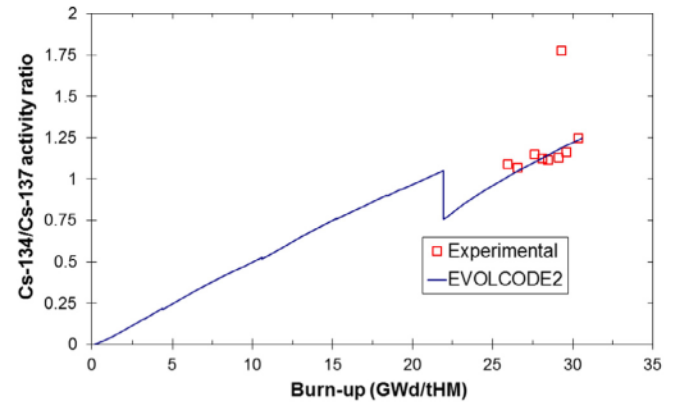


Fig. 18. Comparison of $^{134}\text{Cs}/^{137}\text{Cs}$ activity ratio obtained with EVOLCODE 2.0 and experimental data as function of burn-up.

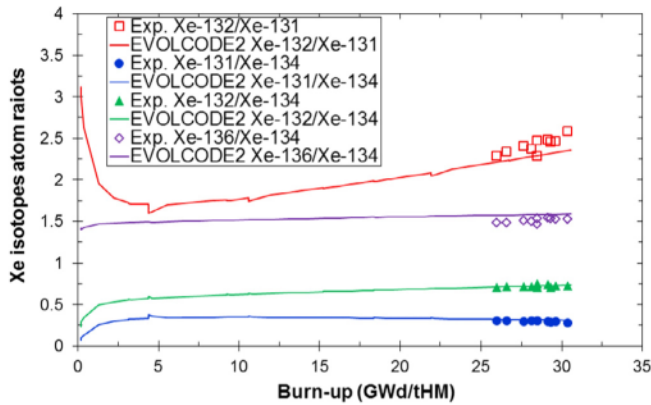


Fig. 16. Comparison of Xe isotopes atom ratios obtained with EVOLCODE 2.0 and experimental data as function of burn-up.

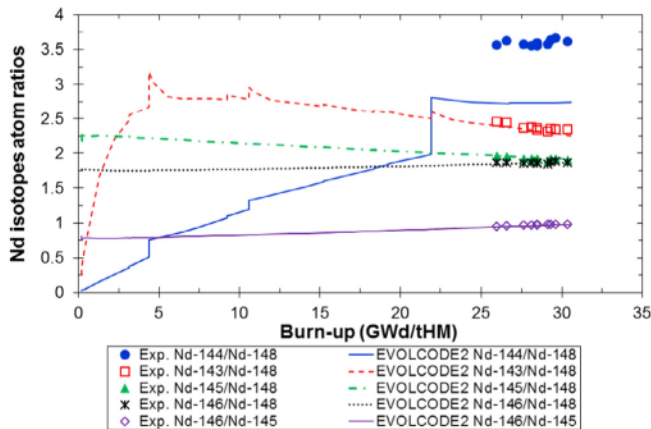


Fig. 17. Comparison of Nd isotopes atom ratios obtained with EVOLCODE 2.0 and experimental data as function of burn-up.

ulation results and the experimental data are larger than the experimental uncertainties, as shown in Table 3. Let us hence apply the theoretical formulation of the S/U analysis developed in Section 2.2 in order to estimate the uncertainties in the isotopic content propagated from the reactions cross sections. This result can provide us with some guidelines in order to understand possible discrepancy sources and to advise additional strategies for cross section uncertainty reduction inside the ANDES project, where this work is framed. In this sense, the methodology applied in this work

also allows estimating the contribution of each energy group to the total uncertainty. These contributions have also been estimated and will be mentioned in the text when appropriate.

The first step is to apply the classical approach consisting in propagating the cross section uncertainties considering only the explicit dependence of the neutron flux on the cross sections. A second step will be taking into account the implicit dependence of the neutron flux normalization in the formulation. Finally, the effect of the geometry model will be assessed. It has to be noted that the methodology described and used here has been developed externally to the EVOLCODE 2.0 system. Implementing it inside EVOLCODE is considered as future work, and the possibility of using ACAB to this purpose will be considered.

4.1. Classical approach

The uncertainties in the final isotopic composition propagated from the cross sections using the abovementioned classical methodology are shown in the fifth column of Table 3. Additionally Table 4 shows the contribution to the variance in the actinide inventory due to the uncertainty in each potentially relevant isotope/cross section after burn-up.

For the main Pu isotopes, uncertainties propagated from the cross sections and simulation-experiment discrepancies are generally smaller than the experimental data uncertainties (excepting ^{238}Pu whose case will be described in detail later), so it is reasonable to believe that the simulation data discrepancies are caused by the dispersions in the experimental measurements. It has to be noted that, for ^{240}Pu and ^{241}Pu , the contribution to the variance of ^{238}U is larger than the contribution of ^{239}Pu . This is a consequence of the saturation in the amount of ^{239}Pu after a certain burn-up (shown in Fig. 7), so that the relevant magnitude to that variance becomes the continual creation of ^{239}Pu (given by captures in ^{238}U) instead of reactions in ^{239}Pu itself.

Each uranium isotope shows a different behaviour. The averaged difference between the simulated and the experimental data for ^{238}U is smaller than the other uncertainty sources. On the contrary, for ^{235}U , the uncertainty propagated from the cross section has a very low value, 0.35%, smaller than the experimental data uncertainty. This indicates that the (small) discrepancy between the EVOLCODE results and the experimental data must be caused for other reasons, possibly: (a) the 4% experimental uncertainty in the burn-up; (b) the impact of considering the implicit dependence of the neutron flux normalization; (c) the complexity of the geometrical model; or (d) an underestimation of ^{235}U reaction uncertainties in the database. The fact that other relevant nuclides do not show this behaviour makes us disregard the possibility that

Table 4

Variance in the isotopic inventory due to the cross sections. Relevant isotope/reaction contributors to the variance are also shown.

Variance (%) due to	Isotope						
	²³⁵ U	²³⁶ U	²³⁸ U	²³⁸ Pu	²³⁹ Pu	²⁴⁰ Pu	²⁴¹ Pu
²³⁵ U (n,f + γ) ¹	100.0	91.6	0.0	1.72	0.0	0.0	0.0
²³⁶ U (n, γ)	0.0	8.4	0.0	14.1	0.0	0.0	0.0
²³⁸ U (n, γ)	0.0	0.0	100.0	0.0	90.4	18.4	53.3
²³⁷ Np (n, γ)	0.0	0.0	0.0	16.5	0.0	0.0	0.0
²³⁸ Pu (n, γ)	0.0	0.0	0.0	67.7	0.0	0.0	0.0
²³⁸ Pu (n,f)	0.0	0.0	0.0	0.0	0.0	0.0	0.0
²³⁹ Pu (n,f + γ)	0.0	0.0	0.0	0.0	9.6	4.8	15.1
²⁴⁰ Pu (n, γ)	0.0	0.0	0.0	0.0	0.0	76.8	6.7
²⁴¹ Pu (n, γ)	0.0	0.0	0.0	0.0	0.0	0.0	5.0
²⁴¹ Pu (n,f)	0.0	0.0	0.0	0.0	0.0	0.0	19.8
Total variance (g ²)	1.00E – 09	4.60E – 09	7.17E – 08	5.78E – 11	3.72E – 09	1.60E – 09	7.40E – 10

¹ For a given isotope, cross correlations between cross sections are so strong that considering these cross sections separately loses sense. In case that the usual procedure is applied separating these cross sections, negative contributions to the variance of some nuclides could appear.

the experimental uncertainty in the burn-up -a)- is responsible. Additionally Table 4 shows that the main contributing reaction to the uncertainty in ²³⁵U is the ²³⁵U (n,f + γ) reactions (the two most thermal groups with a contribution of about 76%). This uncertainty might cause that the burn-up were not well calculated but this result is not shown in the other isotopes so we disregard d) as well. The other possible causes will be explored in the following sections.

For the other isotopes, ²³⁶U and ²³⁸Pu, the averaged deviation between EVOLCODE and experiment is larger than both experimental and cross section uncertainties. Nuclide ²³⁶U has a large experiment-simulation discrepancy (underestimation of around 5.5%) not justifiable by the propagation of the cross section uncertainties (1.8%). According to Table 4, the main contributing reaction to this uncertainty is ²³⁵U (n,f + γ). In (Cao et al., 2010), a similar underestimation for this isotope was found with MCNPX/CINDER for the simulation of ICE. According to this reference, one of the possible factors inducing this discrepancy might be the inconsistency and inaccuracy in the ²³⁵U (n, γ) cross section databases in the energy range of 30 keV to 1 MeV above the resonance range, showing a 10% discrepancy in the capture cross section between libraries. However, according to our S/U analysis, the main contributors to the ²³⁶U uncertainty are the two most thermal groups (see Table 2) from ²³⁵U (n, γ), with a contribution of almost 80% of the total as shown in Fig. 19. This makes us disregard the previous possibility. Unfortunately, this result shows that the COMMARA covariance database is insufficient for a complete S/U analysis of a light water-cooled reactor, since it provides the energy region responsible of the largest uncertainty but not a (small enough) energy group for which the uncertainty should be reduced. On the other hand, this result does provide a real motivation to improve the database subdivision in groups so that this kind of studies can be improved.

As possible sources of this discrepancy, the complexity of the geometrical model (leading to a possible small change in the thermal spectrum with effect in the ²³⁵U (n, γ) resonance centered at 0.027 eV) and the impact of considering the implicit dependence of the neutron flux normalization will be explored in the following sections. It has to be noted that validations made with other different experiments show that the final content of ²³⁶U can be correctly reproduced (San-Felice et al., 2012).

Nuclide ²³⁸Pu also has a simulation-experiment discrepancy (–24%) larger than both the experimental uncertainty (15%) and the cross section-propagated uncertainty (6%). Table 4 shows that the contribution to the cross section-propagated uncertainty due to the parent isotopes (mainly ²³⁶U and ²³⁷Np) is around 32%. The other ~68% is due to the ²³⁸Pu (n, γ) uncertainty, particularly the two most thermal energy groups. The contribution to the

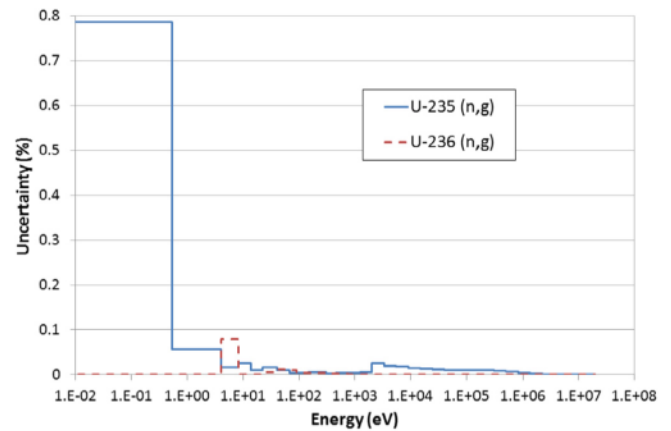


Fig. 19. Contribution to the uncertainty of ²³⁶U per energy group. Given the high correlation, the two groups with lower energies have been joined for this graph. Remaining correlations make the sum of the groups contributions slightly different from 100%.

uncertainty for each isotope and energy group can be seen in Fig. 20. Since ²³⁶U is the gateway for the creation of this isotope, it is reasonable that its amount is underestimated as the parent isotope, although this is not enough to justify the discrepancy between simulation and experiment data. The impact of the complexity of the geometrical model and of considering the implicit dependence of the neutron flux normalization will be explored in the following sections. It should be taken into account that simulation and experimental data are compatible (smaller than 1 sigma considering both abscissa and ordinate) in most points considering all the uncertainties.

4.2. Impact of the implicit dependence of the neutron flux normalization

The sixth column of Table 3 shows the uncertainties in the final inventory considering the implicit dependence of the neutron flux normalization on the cross sections as developed in Section 2.2.2. The different contributions to the variance in the actinide inventory due to the uncertainty in each potentially relevant isotope/cross section after burn-up are shown in Table 5. In this table, the cumulative fission product yields leading to ¹⁴⁸Nd from fissions of ²³⁵U and ²³⁹Pu are also included as additional possible uncertainty sources, since their uncertainty is provided in the JEFF3.1.1 data library. Values for the cumulative fission product yields lead-

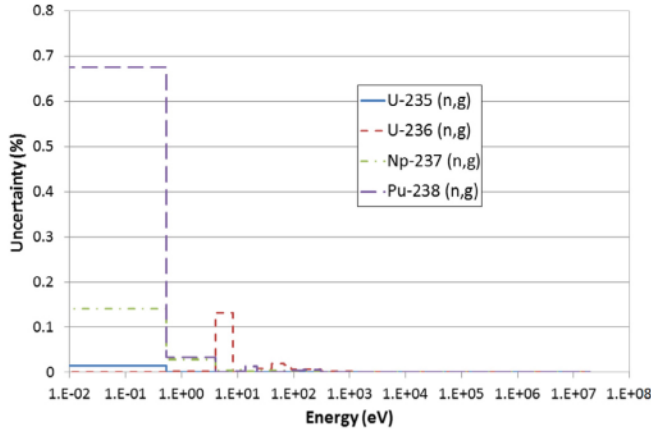


Fig. 20. Contribution to the uncertainty of ^{238}Pu per energy group. Given the high correlation, the two groups with lower energies have been joined for this graph. Remaining correlations make the sum of the groups contributions slightly different from 100%.

ing to ^{148}Nd taken in this work are $1.68 \cdot 10^{-2} \pm 1.2 \cdot 10^{-4}$ and $1.66 \cdot 10^{-2} \pm 1.7 \cdot 10^{-4}$, respectively for ^{235}U and ^{239}Pu .

Some differences arise due to considering the implicit dependence of the neutron flux normalization as shown in this table. Every reaction having an impact in the burn-up has a certain impact in the variance of almost every isotope. These reactions are ^{235}U fission and capture, ^{238}U capture, ^{239}Pu fission and capture and the cumulative fission product yields leading to ^{148}Nd . The main reaction is neutron capture in ^{238}U , having a significant impact in Pu isotopes (as in the classical analysis) but also in the U isotopes. Also, the uncertainties in both cumulative fission product yields leading to ^{148}Nd are also significant, mainly for U isotopes because of their larger dependence with burn-up during the irradiation. This suggests that for a reduction in the impact from the cross section uncertainties, in addition to a reduction in the cross sections uncertainties, it is necessary that the uncertainty in the cumulative fission product yields leading to ^{148}Nd also be reduced.

The main differences regarding the classical approach can be found for the U isotopes, in particular for ^{235}U , with a crucial increase in uncertainty due to cross sections up to 1.2% instead of 0.35%, obtained with the classical methodology. Using the new methodology the uncertainty due to cross sections is larger than the experimental uncertainty (0.65%) and significantly closer to the simulation-experiment discrepancy (with a value of 2.3%), so it helps to explain this discrepancy. In the classical approach, the main contributing reaction to the ^{235}U uncertainty was the ^{235}U

fission reaction. On the contrary, in the new methodology this reaction has minor importance and other contributors arise as ^{238}U capture and the cumulative fission product yields. The addition of the new contributions is the cause of the increase in the ^{235}U final uncertainty, as can be seen in the values of the total variance in this isotope inventory, with an increase of more than an order of magnitude (from 10^{-9} g^2 to $1.32 \cdot 10^{-8} \text{ g}^2$).

For ^{236}U , the uncertainty due to the cross sections also increases, from 1.8% to 2.2%, but it is still not enough to justify the simulation-experiment discrepancy of 5.5%. For ^{238}U and the Pu isotopes (and in particular for ^{238}Pu), this methodology introduces negligible or very small effects.

4.3. Impact of the geometrical model

In this section, the effect of the geometry model in the simulation of the ICE experiment is assessed. A more sophisticated geometry (as a fuel assembly slice) has been implemented as described in Section 2.3.2. Results with this geometry model are included in Table 3, column four. As shown in the table, this geometry model has a significant impact for the fissile species ^{235}U , ^{239}Pu and ^{241}Pu , and negligible impact for the others. For these isotopes the averaged difference between the simulation results and the experimental data is considerably reduced regarding the simulation with the pin model, meaning that the energy spectrum of the neutron flux is better estimated.

For the particular case of ^{235}U , the averaged simulation-experiment discrepancy is reduced from 2.3% to 1.8%, compatible (smaller than 1 sigma) with the experimental uncertainty plus the full uncertainty from nuclear data. For ^{239}Pu , the new value of the simulation-experiment discrepancy is equal to the uncertainty coming from the cross sections, meaning that this isotope is excellently reproduced with this geometry model. For the other fissile species, ^{241}Pu , the averaged simulation-experiment difference using the pin model was already similar to the experimental uncertainty and the cross section uncertainty.

For the particular cases of ^{236}U and ^{238}Pu , no significant effect is found from the use of this alternative geometrical model.

4.4. Discussion

In the previous sections we have analyzed in depth the cases of those isotopes (^{235}U , ^{236}U and ^{238}Pu) for which the difference between the EVOLCODE results and the experimental data is larger than the other uncertainty sources. In particular, we have explored separately the possible impacts of considering the implicit dependence of the neutron flux normalization in the S/U analysis and the

Table 5

Variance in the isotopic inventory due to the cross sections considering the neutron flux normalization. Relevant isotope/reaction contributors to the variance are also shown.

Variance (%) due to	Isotope						
	^{235}U	^{236}U	^{238}U	^{238}Pu	^{239}Pu	^{240}Pu	^{241}Pu
^{235}U (n,f + γ)	8.2	66.3	2.1	2.0	0.0	0.0	0.3
^{236}U (n, γ)	0.0	5.7	0.0	13.3	0.0	0.0	0.0
^{238}U (n, γ)	34.2	10.4	44.3	2.0	90.1	16.0	33.3
^{237}Np (n, γ)	0.0	0.0	0.0	15.5	0.0	0.0	0.0
^{238}Pu (n, γ)	0.0	0.0	0.0	63.9	0.0	0.0	0.0
^{238}Pu (n,f)	0.0	0.0	0.0	0.0	0.0	0.0	0.0
^{239}Pu (n,f + γ)	2.5	0.8	2.3	0.1	9.9	5.2	21.6
^{240}Pu (n, γ)	0.0	0.0	0.0	0.0	0.0	78.6	7.9
^{241}Pu (n, γ)	0.0	0.0	0.0	0.0	0.0	0.0	6.0
^{241}Pu (n,f)	0.0	0.0	0.0	0.0	0.0	0.0	23.4
$\gamma_{\text{Nd}148}$ from ^{235}U	34.8	10.6	32.3	2.0	0.02	0.1	4.8
$\gamma_{\text{Nd}148}$ from ^{239}Pu	20.3	6.2	18.9	1.2	0.01	0.1	2.8
Total (g^2)	$1.32\text{E} - 08$	$6.75\text{E} - 09$	$4.75\text{E} - 08$	$6.13\text{E} - 11$	$3.63\text{E} - 09$	$1.56\text{E} - 09$	$6.27\text{E} - 10$

complexity of the geometrical model. In this section, a general discussion for each isotope will be made.

Although Table 3 shows the information about the experimental, simulation and cross section-propagated uncertainties, this information is also shown in Fig. 21 to improve understandability. For each isotope, the grey area represents the experimental uncertainties. Two points are included for each isotope as well. The one to the left represents the averaged difference (in %) between the simulation results and the experimental data using the pin model and the one to the right shows this value for the assembly geometry model. Surrounding each point, the squared area represents the uncertainty due to the cross sections applying the classical model while the error bars represent the cross section uncertainty applying the new methodology, i. e., taking into account the implicit dependence of the neutron flux normalization in the cross sections uncertainty. This has been calculated only for the pin model. For the case of ^{235}U , the pin model uncertainty bar has also been drawn in the figure as an extrapolation for the assembly model in order to show every possible uncertainty for that case.

For ^{235}U , the uncertainty propagated from the cross section using the classical methodology has a very low value, 0.35%, smaller than the experimental data uncertainty of 0.65% and the simulation-experiment difference of 2.3%. On the one hand, taking into account the implicit dependence of the neutron flux normalization, the uncertainty propagated from the cross sections rises to 1.2% due to the additional contributions to the ^{235}U variance of the uncertainties propagated from ^{238}U capture and the cumulative fission product yields leading to ^{148}Nd . On the other hand, the simulation using a geometry model of an assembly slice provides a smaller simulation-experiment difference of 1.8% since the energy spectrum of the neutron flux is better estimated. Considering each of these calculations alone, none is enough to explain why the simulation-experiment difference is larger than the experimental uncertainty. However, when both rationales are taken into account together, the simulation-experiment difference is of the same order of magnitude that the uncertainty propagated from the cross sections, and compatible with the experimental uncertainty.

Regarding ^{236}U , the experiment-simulation difference (-5.5%) is larger than the experimental uncertainty (0.92%) and the uncertainty due to the cross sections (1.8%). According to our S/U analysis, the main contributors to the ^{236}U uncertainty are the two most thermal groups from ^{235}U (n, γ), with a contribution of almost 72% of the total. It has to be mentioned that this energy group subdivision in the thermal region is insufficient for a complete S/U

analysis of a light water-cooled reactor, since it provides the energy region responsible of the largest uncertainty but not a (small enough) energy group for which the uncertainty should be reduced. This result should be seen as a real motivation to improve the database subdivision in groups so that this kind of studies can be improved. Considering the implicit dependence of the neutron flux normalization in the calculations, the uncertainty due to the cross sections rises to 2.2%, still a small value compared with the experiment-simulation discrepancy. Besides, the simulation using a geometry model of an assembly slice provided an averaged experiment-simulation discrepancy very close to the pin-model one, -5.4% . As a conclusion, the source of the averaged experiment-simulation discrepancy of ^{236}U cannot be explained with the procedures used here. Although it has been shown in the bibliography that the final content of this isotope can be correctly reproduced with simulations in other experiments, for the ICE experiment similar underestimation for this isotope have been found with other simulation codes. This issue requires further research.

A similar conclusion can be achieved for ^{238}Pu . In this case, the averaged experiment-simulation difference of -24% is larger than both the uncertainty due to the cross sections (6.0%) and the experimental uncertainty (15%). Since ^{236}U is the gateway for the creation of this isotope, it is reasonable that the amount of ^{238}Pu is underestimated as the parent isotope (-5.5%), although this does not fully justify the observed discrepancy. Neither considering the implicit dependence of the neutron flux normalization nor making a simulation with an assembly model help to explain this issue, since these methodologies provide values of the uncertainties very similar to the previous ones. It has to be noted that a similar underestimation in the final amount of this isotope was also found in other simulations of this experiment involving MCNPX/CINDER or KAPROS. It should also be taken into account that simulation and experimental data are compatible (1.5 sigmas) considering the error bar assigned to the atom densities and to the experimental burn-up points. However, results for this isotope require further research.

For the other nuclides, ^{238}U , ^{239}Pu , ^{240}Pu and ^{241}Pu , the figure shows that simulation and experimental values are compatible within the experimental and the cross section uncertainties, showing even better agreement in the case of the simulation with an assembly model for the fissile isotopes. For the minor actinides Am and Cm, although they have not been included in this analysis, we have found similar results to those published in bibliography.

5. Conclusions

The ICE experiment has been satisfactorily simulated using the EVOLCODE 2.0 simulation system as an on-going effort to validate and upgrade this tool. Despite the very simple geometrical model of the reactor, the agreement between calculated and experimental data is excellent for most actinides, mainly those with a larger amount, and also for many fission products, compared as isotope ratios.

In particular for the uranium isotopes, the agreement is very good for ^{235}U (difference of 2.3% with experimental data) and excellent for ^{238}U (0.023%). For the plutonium isotopes, the agreement between the simulation and the experimental data is very good as well, with differences smaller than 3% for the main isotopes. On the other hand, discrepancies larger than experimental and cross sections induced uncertainties appear for ^{236}U and ^{238}Pu (around -5.5% and -23% respectively). Similar results can be however found in bibliography for these isotopes in other simulations of this experiment.

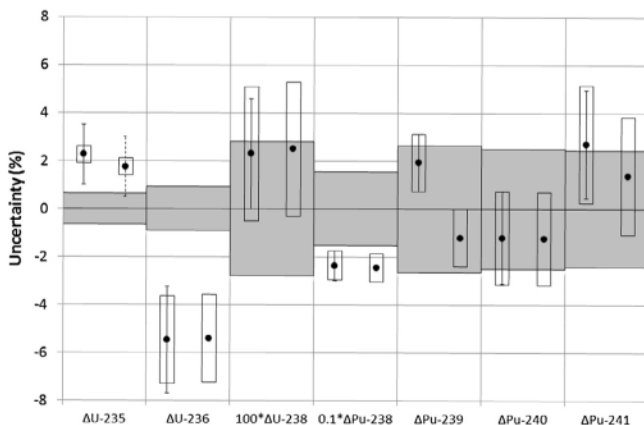


Fig. 21. Uncertainty in the final inventory due to experimental data (grey area), simulation-experiment discrepancy (for each isotope, the point to the left show the result for the pin model and the point to the right is for the assembly model), and uncertainty due to cross sections (squares represent the uncertainty using the classical method and error bars show the uncertainty with the implicit effect in flux normalization).

For fission products, we have found that the simulation with EVOLCODE reproduces very satisfactorily the experimental isotope ratios for Kr, Xe and Nd elements and for the $^{134}\text{Cs}/^{137}\text{Cs}$ activity ratio. More than that, we have provided some hints for the improvement of both the JEFF3.1.1 fission yield library and the experimental results. In particular, fission yields leading to ^{84}Kr seem to be underestimated in the database, since both isotope ratios $^{84}\text{Kr}/^{83}\text{Kr}$ and $^{84}\text{Kr}/^{86}\text{Kr}$ are equally underestimated ($\sim 18\%$) while $^{83}\text{Kr}/^{86}\text{Kr}$ atom ratio, with no presence of ^{84}Kr , has a discrepancy of only $\sim 1.24\%$.

Concerning the experimental results, data for Kr ratios shows an inconsistency suggesting that the values of $^{83}\text{Kr}/^{86}\text{Kr}$ have to be divided by a factor 10. Additionally, although the experiment description states that experimental results were corrected to the date of the reactor shutdown, results suggest that the amounts of ^{144}Nd at the time of the experimental measure were not corrected, since the values of $(^{144}\text{Nd}+^{144}\text{Ce})/^{148}\text{Nd}$ taken from the simulation show a discrepancy with experimental data of only $\sim 4\%$ instead of -24% for the amount of $^{144}\text{Nd}/^{148}\text{Nd}$.

In addition, a Sensitivity/Uncertainty analysis considering the cross sections uncertainties and correlations was developed to analyze the origin of the remaining discrepancies between the EVOLCODE results and the experimental data of the ICE experiment. For most isotopes, uncertainties propagated from the cross sections and simulation-experiment differences are generally smaller than the experimental data uncertainties, so the simulation-experiment differences are caused by the dispersions in the experimental measurements.

The difference between the EVOLCODE results and the experimental data is larger than the estimated uncertainty for these isotopes: ^{235}U , ^{236}U and ^{238}Pu . To analyse their cases in depth, a new methodology in the S/U analysis has been developed, accounting for the implicit dependence of the neutron flux normalization. Additionally, the complexity of the geometrical model has also been assessed.

The improved S/U methodology, neglected in this kind of studies, has proven to be an important contribution to the explanation of the difference between the simulation and the experimental data of ^{235}U . The uncertainty propagated from the cross sections increases from 0.35% to 1.2% due to the additional contributions of the uncertainties propagated from ^{238}U capture and the cumulative fission product yields leading to ^{148}Nd (both cumulative fission product yields leading to ^{148}Nd are significant for U isotopes because of their larger dependence with burn-up during the irradiation). Uncertainties from reactions having an impact in the burn-up have proven to impact in the variance of almost every isotope. Besides, the simulation using a geometry model of an assembly slice provides a smaller simulation-experiment difference of 1.8% since the energy spectrum of the neutron flux is better estimated. Taking both elements together the ^{235}U estimation from EVOLCODE becomes compatible with the experimental data for the ICE experiment.

For the cases of ^{236}U and ^{238}Pu , no significant improvement was found neither from the use of the new methodology nor from the alternative geometrical model. On the other hand, for the ICE experiment similar underestimations have been found with other simulation codes, although it has been shown in the bibliography that the final content of these isotopes can be correctly reproduced with simulations in other experimental benchmarks. This issue requires further research.

Additionally, the reaction and energy group responsible of the uncertainties have also been estimated for these isotopes. However, the energy group subdivision in the thermal region is not enough to suggest a small enough energy group for which a reduction in its reaction cross section uncertainty. This issue should be

seen as a motivation to improve the database subdivision in groups so that this kind of studies can be improved.

Finally, it can be concluded that the EVOLCODE 2.0 simulation system is able to reproduce satisfactorily the isotopic composition of a PWR, even with a simple geometrical model. In the ICE experiment the burn-up reached around 30 GWd/tU. Other experimental data are required for the validation of the code for deeper burn-up simulations.

Acknowledgements

Authors would like to acknowledge ENRESA (as part of the CIE-MAT-ENRESA collaboration) and the 7th FP of the EU ANDES project for partially supporting this work.

References

- Aliberti, G., Palmiotti, G., Salvatores, M., Stenberg, C.G., 2004. Impact of nuclear data uncertainties on transmutation of actinides in accelerator-driven assemblies. *Nucl. Sci. Eng.* 146, 13–50.
- Álvarez-Velarde, F., 2011. Development of a Computational Tool for the Simulation of Innovative Transmutation Systems (Ph.D. thesis). University of Córdoba, Spain. <http://helvia.uco.es/xmlui/handle/10396/4461>.
- Álvarez-Velarde, F., González-Romero, E.M., 2011. Validation of the Burn-up Code EVOLCODE 2.0 with PWR Spent Fuel Compositions. In: *Proceeding of GLOBAL2011* (Makuhari, Japan). Paper No. 360438.
- Álvarez-Velarde, F., León, P.T., González-Romero, E.M., 2007. EVOLCODE2, a Combined Neutronics and Burn-up Evolution Simulation Code. In: *Proc. 9th Information Exchange Meeting on Actinide and Fission Product P&T* (Nîmes, France), ISBN 978-92-64-99030-2, NEA/OECD.
- ANDES, 2010. Accurate Nuclear Data for nuclear Energy Sustainability. In: *EU 7th Framework Programme, Contract Proposal N° 249671*.
- Barbero, P., Bidoglio, G., Caldiroli, A., Daniele, F., de Meester, R., Ernstberger, R., Fachetti, S., Frigo, A., Guardini, S., Guzzi, G., Hansen, P., Lezzoli, L., Koch, L., Konrad, W., Mammarella, L., Mannone, F., Marelli, A., Schurenkamper, A., Trincerini, P.R., Wellum, R., 1979. Postirradiation Analysis of the Obrigheim PWR Spent Fuel, EUR 6589e.
- Broeders, C.H.M., 1992. Entwicklungsarbeiten für die neutronenphysikalische Auslegung von Fortschrittlichen Druckwasserreaktoren (FDWR) mit kompakten Dreiecks-gittern in hexagonalen Brennelementen. Technical report KfK5072, Kernforschungszentrum Karlsruhe – Institut für Neutronenphysik und Reaktortechnik. <http://inrwww.webarchiv.kit.edu/kfK5072.html>.
- Broeders, C.H.M., Cao, Y., Gohar, Y., Álvarez-Velarde, F., 2010. Isotope Correlation Experiment in NPP Obrigheim. IAEA CRP ADS Research, Subtask Reactor Fuel Burn-up Qualification/Validation.
- Broeders, C.H.M., Dagan, R., Sanchez, V., Travleev, A., 2004. KAPROS-E: Modular Program System for Nuclear Reactor Analysis, Status and Results of Selected Applications, Reaktortagung Duesseldorf. http://inrwww.webarchiv.kit.edu/pdfs/ktp2004_kapros.pdf.
- Brown, F., Kiedrowski, B., Bull, J., 2010. MCNP5-1.60 Release Notes. Los Alamos National Laboratory, LA-UR-10-06235.
- Cao, Y., Gohar, Y., Broeders, C.H.M., 2010. MCNPX Monte Carlo burnup simulations of the isotope correlation experiments in the NPP Obrigheim. *Ann. Nucl. Energy* 37, 1321–1328.
- Croff, A.G., 1980. A User's Manual for the ORIGEN2 Computer Code, ORNL/TM-7175.
- Croff, A.G., 1983. ORIGEN2: a versatile computer code for calculating the nuclide compositions and characteristics of nuclear materials. *Nucl. Technol.* 62 (3), 335–352.
- Fensin, M., Hendricks, J., McKinney, G.W., Trellue, H., 2006. Advances in Monte Carlo Depletion Capabilities for MCNPX. In: *American Nuclear Society's 14th Biennial Topical Meeting of the Radiation Protection and Shielding Division*.
- Furcola, N.C., 1996. Standard Test Method for Atom Percent Fission in Uranium and Plutonium Fuel (Neodymium-148 Method). *Annual books of ASTM Standards* 12.02, E321–96.
- García-Herranz, N., Cabellos, O., Álvarez-Velarde, F., Sanz, J., González-Romero, E.M., Juan, J., 2010. Nuclear data requirements for the ADS conceptual design EHT: uncertainty and sensitivity study. *Ann. Nucl. Energy* 37, 1570–1579.
- García-Herranz, N., Cabellos, O., Sanz, J., González-Romero, E.M., Juan, J., Kuijper, J.C., 2008. Propagation of statistical and nuclear data uncertainties in Monte Carlo burn-up calculations. *Ann. Nucl. Energy* 35, 714–730.
- Haack, W., Verboomen, B., 2007. An optimum approach to Monte Carlo burn-up. *Nucl. Sci. Eng.* 156, 180–196.
- Herman, M., Obložinský, P., Mattoon, C.M., Pigni, M., Hoblit, S., Mughabghab, S.F., Sonzogni, A., 2011. COMMARA-2.0 Neutron Cross Section. Covariance Library. National Nuclear Data Center BNL-94830–2011, March.
- Janczysyn, J., Pohorecki, W., Domanska, G., Taczanowski, S., Maiorino, R.J., David, J.-Ch., Álvarez-Velarde, F., 2011. Benchmark on Radionuclides Production and Heat Generation Rates in Lead Targets Exposed to 660 MeV Protons. AGH University of Science and Technology, ISBN 978-83-911589-0-6, Krakow.

- Koch, J L., Schoof, S, 1981. The Isotope Correlation Experiment ICE – Final Report, Technical Report Nr, 2/81 (KfK3737), ESARDA.
- Pelowitz, D.B., Hendriks, J.S., Durkee, J.W., James, M.R., Fensin, M.L., McKinney, G.W., Mashnik, S.G., Waters, L.S., 2009. 'MCNPX 2.7.A Extensions, LA-UR-08-07182, Los Alamos National Laboratory.
- San-Felice, L., Eschbach, R., Bourdot, P., Tsilanizara, A., Huynh, T.D., Ourly, H., Thro, J.F., 2012. Experimental validation of the DARWIN2.3 package for fuel cycle applications. PHYSOR 2012 – Advances in Reactor Physics – Linking Research, Industry, and Education, Knoxville, Tennessee, USA, April 15–20.
- Sanz, J., Cabellos, O., García-Herranz, N., 2008. ACAB Inventory Code for Nuclear Applications: User's Manual, Version 2008. <https://rsicc.ornl.gov/codes/ccc/ccc7/ccc-758.html>.
- Send, L., 2005. Investigations for Fuel Recycling in LWRs (Ph.D. thesis). Karlsruhe, Germany. in www.webarchiv.kit.edu/pdfs/thesis_send.pdf.